The Structures of Integrins and Integrin–Ligand Complexes: Implications for Drug Design and Signal Transduction

Kay-E. Gottschalk and Horst Kessler*

Integrins are pivotal proteins in cell–cell adhesion, signaling and apoptosis. These properties render them attractive targets for drugs, especially those involved in cancer treatment. Recently, the structures of the extracellular domains of one of the integrin subtypes was solved with X-ray crystallography in the free form as well as bound to a ligand. These structures in combination with NMR spectroscopic data, electron microscopy images, and molecular modeling provide deeper insight into the mechanism of integrin-mediated signal transduction. The structures make structure-based rational drug design possible and are certainly hallmarks in integrin research.

1. Introduction

In the postgenomic era it has become a common approach for drug development to specifically block the function of certain previously identified key proteins in signal pathways. Membrane-spanning receptors such as G protein-coupled receptors (GPCR), ion channels or integrins constitute the majority of drug targets. The biggest dilemma in rational drug design for these kinds of targets is the lack of sufficient high-resolution structural information of the involved proteins. A number of recent structural studies on integrins shed new light on the background of ligand binding and signal transduction of this highly important class of proteins.

Integrins are involved in a large number of fundamental cellular processes such as cell-matrix adhesion, differentiation, proliferation, apoptosis (natural cell death), and stress response.[1] They couple intracellular signals with extracellular responses and vice versa. Integrins consist of two noncovalently bound subunits, an α and a β subunit. Different subunit combinations confer different specificities for extracellular ligands.

A large number of pathways have been connected with integrin function.[2] Integrins are pivotal proteins in cell–cell communication which are connected to many regulatory phenomena. They can interact with the extracellular matrix as well as with proteins of the same cell, for example, the urokinase receptor uPAR. Furthermore they are involved in many common diseases. One major reason for the interest of researchers in pharmaceutical companies and academia alike is the fact that certain classes of integrins are overexpressed in tumor cells, rendering them attractive antitumor targets.[3, 4] Herein we describe how structural information on integrins can shift drug design attempts from ligand-based rational design to protein-based rational design, and on how different techniques, namely biochemical investigations, X-ray diffraction, and NMR spectroscopy in combination with electron microscopy and molecular modeling provide new insight into signal transduction by integrins.

[*] Prof. Dr. H. Kessler, K.-E. Gottschalk
Institut für Organische Chemie und Biochemie
Technische Universität München
Lichtenbergstraße 4 (Germany)
Fax: (+49) 89-289-13210
E-mail: horst.kessler@ch.tum.de

2. Structure of the Extracellular Domains of $\alpha_v\beta_3$ Integrins

Integrins are heterodimeric receptors that are composed of large extracellular domains, one transmembrane (TM) helix, and small intracellular domains per subunit.[5] Recently, the structure of the extracellular domains of $\alpha_v\beta_3$ has been solved in a pioneering work by Xiong et al.[6] In accordance with earlier electron-microscopy (EM) work,[7] it has been shown that integrins consist of an ovoid head and two linear stalk regions. In contrast to the EM studies, these tails are severely bent at defined regions (Figure 1, left). This flexibility might be a crystallization artifact or related to integrin function. As the head groups of integrins have been identified as the major ligand-binding regions, their structure is of primary interest for drug design (Figure 1, right).

The head domain of the α subunit consists of a seven-bladed β propeller; each blade is formed by a four-stranded antiparallel β sheet (Figure 2, top). The βA domain of the β subunit assumes a Rossmann fold, which is also found in Gβ domains and αA domains of integrins. Helices surround a central six-stranded β sheet (Figure 2, middle). The central interfacial residue appears to be the Arg 261 of the β subunit, which inserts into the β propeller of the α subunit and stabilizes the complex by cation–π interactions (Figure 2, bottom).

  1433-7851/02/4120-3767 $ 20.00+.50/0

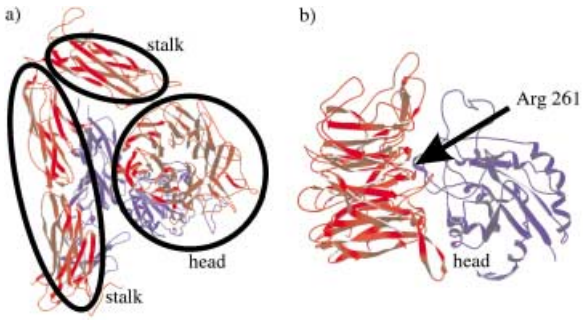

Figure 1. Crystal structure of the extracellular domains of integrin $\alpha_v\beta_3$. a) The α subunit is shown in red, the β subunit in blue. A kink in the stalk regions can be observed, which is not in accordance with EM images. b) Head groups: In accordance with EM images, the head group of $\alpha_v\beta_3$ has an ovoid form. A tight interface is formed, with (β)-Arg261 inserting into the β propeller of the α subunit.

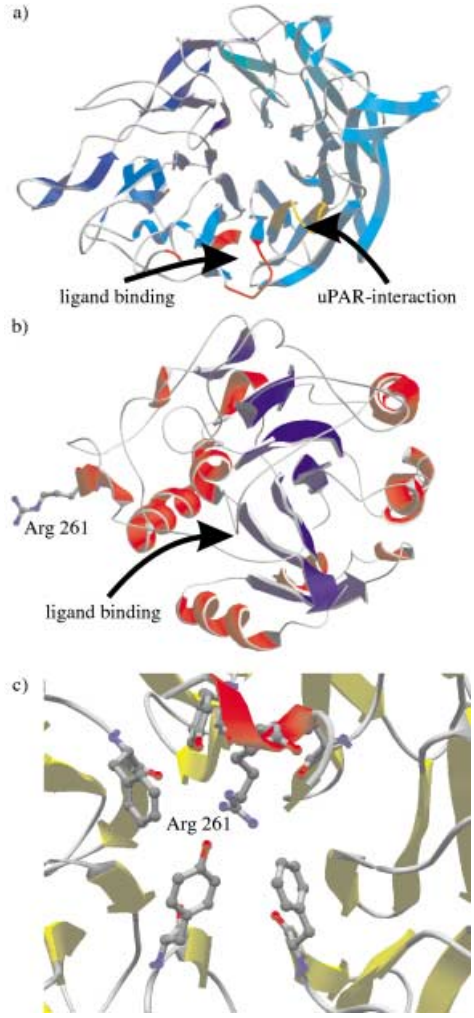

Figure 2. The interface of the head groups. a) The β propeller of the α subunit. The N-terminal domain of the α subunit forms a seven-bladed β propeller. The loops that are affected by ligand binding or by interactions with the urokinase receptor uPAR (in the case of $\alpha_3\beta_2$) are colored red and orange, respectively. b) The βA domain of the β subunit. Arg261 inserts into the β propeller of the α subunit. Ligand binding occurs close to Arg261. c) Cation–π interactions between Arg261 of β_3 (red) and surrounding aromatic residues of α_v (yellow) stabilize the head-group interactions. Cation–π interactions are ideally suited to fine tune protein–protein interfaces: Slight changes in the position of the involved residues can render these interactions repulsive, inducing large conformational changes.

3. Structure of the Integrin–Ligand Complex

According to an X-ray structure analysis of the integrin ligand complex,[9] the overall structure does not change very much after binding of c(-RGDf[NMe]V-)[8] as ligand. This might be caused by crystal contacts, which inhibit large movements. The root-mean-square deviation between the head groups of the free and complexed form is smaller than 1 Å. The α subunit does not change; the main changes are at the β subunit close to the ligand-binding site. A previously unoccupied MIDAS region (MIDAS = metal-ion-dependent adhesion site) now becomes occupied, and a loop nearby shifts towards the α subunit, allowing interactions of the ligand with both subunits. The aspartic acid residue of the RGD ligand binds to the metal ion in the MIDAS region. The only residue of the ligand that is in contact with the α subunit is the arginine, which binds to a region of negative charge in α_v.

An unusual feature of the ligand-binding site is that essentially no hydrophobic interactions can be observed (Figure 3, top). Only D-Phe of c(-RGDf[NMe]V-) is involved in some hydrophobic interactions. The central glycine residue lies directly on the integrin surface and might also add to the stability of the complex. Any substitution of the glycine unit (e.g., by Ala or D-Ala) destroys $\alpha_v\beta_3$-binding activity.[10] The main interactions are between the positively charged arginine and negatively charged side chains in the α subunit and between the anionic aspartic acid and the metal cation in the MIDAS region of the β subunit. Further stabilization occurs through hydrogen bonds between the NH group of Gly-Asp amide bond and the carbonyl oxygen atom of (β)-R216 as well as between the Asp side chain and the NH group of (β)-N215 (Figure 3, bottom). This confirms earlier observations

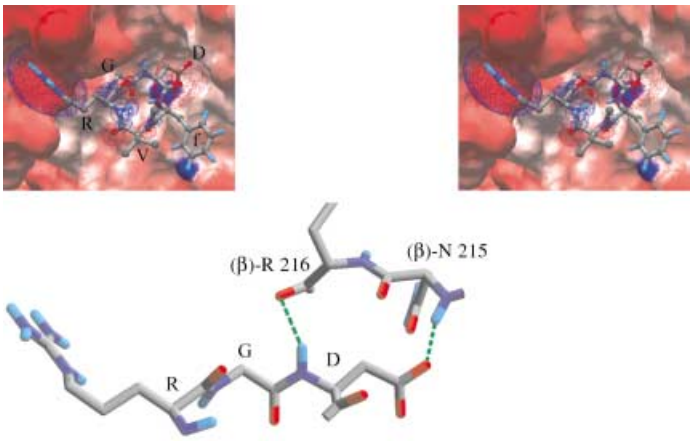

Figure 3. Structure of the crystalline complex. Top: Stereoview. Interactions of c(-RGDf[NMe]V-) with $\alpha_v\beta_3$. The ligand appears to interact mainly through electrostatic forces. R and D form a charged clamp that attaches to regions with opposite charges in the protein: Asp interacts with a metal cation in the β subunit, Arg with two Asp of the α subunit. Gly forms close contact with the proteins surface, D-Phe is involved in hydrophobic interactions. Neither the *N*-methyl moiety nor the side chain of (NMe)V form any contact with the protein. Bottom: The interaction is further stabilized by hydrogen bonds involving the backbone of the protein and the ligand. The NH of Asp forms a hydrogen bond with the oxygen atom of the carboxy group of (β)-Arg261, whereas the Asp side chain not only complexes the metal ion in the MIDAS region, but furthermore forms a hydrogen bond with (β)-N215. MIDAS = metal-ion-dependent adhesion site

  1433-7851/02/4120-3768 $ 20.00+.50/0 *Angew. Chem. Int. Ed.* **2002**, *41*, No. 20

on retro-inverso peptides, which demonstrated the participation of the ligand backbone in binding.[11]

The cleft in which the ligand resides is rather shallow, and large parts of the ligand make virtually no contact with the protein. It seems as if the Asp and Arg residues of the RGD ligand act as an electrostatic clamp, attaching to charged regions of the protein; usually ligands tend to attach to hydrophobic pockets with large interfaces determined by van der Waals interactions.

4. Docking Studies on Free $\alpha_v\beta_3$ Integrin

Prior to the publication of the X-ray crystal structure of the integrin complex, docking studies starting from the crystal structure of the free $\alpha_v\beta_3$ integrin tried to predict the conformational changes accompanying the ligand-binding event.[12] The docking studies were based on the following considerations: in extensive ligand-based rational design studies (the so-called "spatial screening") selectivity between different α as well as β subtypes of integrins was achieved.[13] Although initially the focus was on discriminating between $\alpha_v\beta_3$ and $\alpha_{IIb}\beta_3$, later studies also achieved specificity for $\alpha_v\beta_3$, $\alpha_v\beta_5$, and $\alpha_v\beta_6$.[14] It was further possible to distinguish between the non-RGD-binding integrins $\alpha_4\beta_1$ and $\alpha_4\beta_7$.[15] This implies that the ligands interact with both subunits.

It was postulated earlier that Ca^{2+} bound to the MIDAS region of the αA domain of the integrin subunit β_3 interacts with the aspartic acid residue of RGD peptides and the receptor.[5, 16, 17] Surprisingly, in the crystal structure of free $\alpha_v\beta_3$ the MIDAS region of αA is not populated by a metal ion, as opposed to the neighboring adMIDAS region. Further studies showed that the N-terminal β propeller of the α subunits are also involved in the binding process of ligands and that the arginine residue of RGD binds in this region.[18, 19] Although the distance between the arginine and aspartic acid residues in cyclic RGD peptides is about 13 Å,[9] the shortest distance between the Ca^{2+} bound to the adMIDAS region and the β propeller of the α_v subunit is in the order of 17 Å. Superposition of the βA domain of β_3 and of the I domain of integrin α_2 reveals a high structural similarity between these two structures (Figure 4).[12] Analysis of the structures of the free I domain of α_2 and the I domain in complex with collagen shows that the binding of the ligand results in a movement of the Ca^{2+} ion and the MIDAS region of the I domain.[20] Assuming a similar structural change in β_3 as a working hypothesis enabled similar structural changes in β_3 to be modeled and an RGD mimetic to be docked to the modeled receptor conformation prior to the publication of the structure of the receptor complex with a cyclic RGD peptide.

5. Comparison of the Results of Docking Studies with Those of an X-ray Crystal Structure Analysis of Ligand-Bound Integrin

A comparison between the predicted and the experimentally observed protein and ligand conformation underlines the power of docking studies with human intervention. The trend

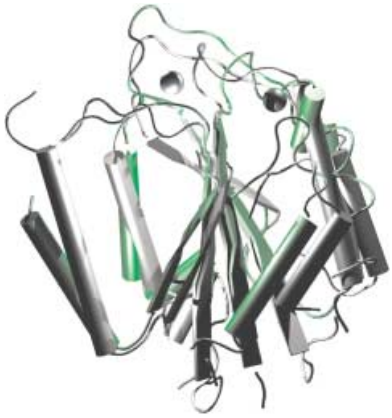

Figure 4. Superposition of the I domain of the collagen-associated integrin subunit α_2 (grey) with the βA domain of the integrin subunit β_3 (green). The respective metal ions are depicted as spheres; the grey sphere represents the metal ion bound to the MIDAS region of α_2, the green sphere the ion bound to the adMIDAS region of β_3. The root-mean-square deviation of the backbone of the superimposed residues is 1.6 Å despite the large difference in metal position.

in the loop change has been predicted correctly, though the model overestimated the structural change (Figure 5, left). The ligand-binding metal ion is nearly at the correct position. As the main interaction of the aspartic acid of the ligand with the integrin takes place through this metal ion, the correct

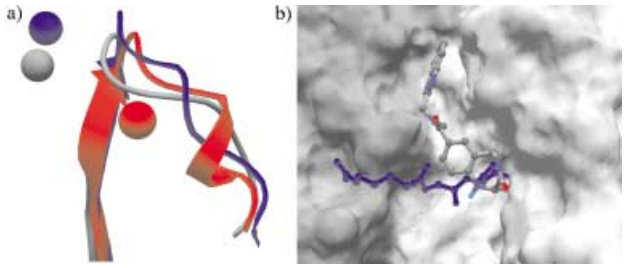

Figure 5. Structural comparison between experimentally determined and calculated structures. a) Comparison of the loop structure and metal position between the free (red) conformation of $\alpha_v\beta_3$, the ligand-bound (blue) conformation, and the modeled (grey) conformation. The main trend in loop change was predicted correctly, although the model overestimates the structural changes. The positions of the metal ions in the modeled form and the ligand-bound form are very similar. b) Comparison of the RGD orientation of the ligand in the crystal and the orientation of the docked ligand. Whereas the carboxy group is positioned nearly identically, the arginine moiety points to a different direction than the arginine mimetic of the docked ligand. This might be either be caused by errors in the docking procedure or by the different nature of the ligand.

positioning of this ion leads to a correct orientation of the acid moiety of the docked peptidomimetic. The arginine mimetic in the bound ligand adopts a different orientation than the Arg in the crystal (Figure 5, right). This might either be a result of the different nature of the ligand or of errors in the docking procedure. Interestingly, the errors in the loop conformation of the modeled integrin structure do not lead to an incorrect orientation of the acid moiety, as only the position of the metal ion seems to be important. This corroborates the above-mentioned assumption that in the

  1433-7851/02/4120-3769 $ 20.00+.50/0

case of RGD peptides the ligand protein interactions are determined by electrostatic interactions.

The differences in the ligand orientation resulting from both studies stress that an experimentally determined structure of the complex with a ligand is essential for rational drug design, especially if conformational changes upon ligand binding are expected to occur. Purely computational studies on the other hand can model trends in conformational changes correctly and can identify ligand-binding regions even in these modeled structures. But the results from these studies have to be regarded as a first approximation.

6. From Ligand-Based Design to Protein-Based Rational Drug Design

Extensive screening studies with cyclic RGD peptides without the knowledge of the protein structure have led to the development of superactive and selective RGD-based cyclic peptides.[21, 22] With the structure of the ligand-bound integrin now available, these results can be interpreted in structural terms, especially as many of the synthesized peptides have been characterized by NMR spectroscopy.

The backbone conformation of the ligand in the crystals of the ligand–integrin complex[9] and in solution determined by NMR spectroscopy in water[23] are very similar (Figure 6, top); particularly the crucial distances between the C_α atoms

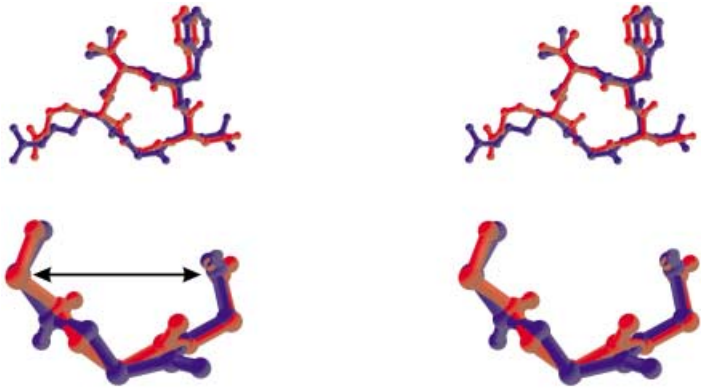

Figure 6. Stereoview of the conformation of c(-RGDf[NMe]V-) bound to the protein (red) and in the free state in aqueous solution (blue). The conformations are identical within the experimental error of the two structures. Especially the crucial C_α distance does not alter upon binding.

of the Arg and Asp residues are identical (Figure 6, bottom).[24, 25] As the X-ray structure is only refined at 3.1-Å resolution, a detailed discussion of the differences in the two structures would not be meaningful. This demonstrates the power of NMR spectroscopy in the determination of the structures of conformationally restricted cyclic peptides in solution[26] without the danger of crystal artifacts. It furthermore stresses the validity of the ligand-based design strategy: one goal is the creation of a rigid scaffold that does not change the conformation upon binding to the receptor. A rigid scaffold has two key advantages: the ligand always adopts the correct conformation, thus there is no equilibrium between different conformations, which would slow down the ligand binding, and the entropic cost is minimized.[26] If bound water is displaced, as may well be the case in a predominantly charged ligand-binding site, binding of ligand might actually be enhanced by an entropy gain.

Screening of different side chains at the Val and D-Phe positions of c(-RGDf[NMe]V-) revealed that in the case of $\alpha_v\beta_3$, Val can be replaced by many moieties of variable size.[10] In the crystal, Val does not make any contact with the protein. Substitution of D-Phe by D-Trp increases the binding affinity, whereas D-Pro disables binding.[10] Superposing the NMR-derived structures of the respective RGD peptides with the X-ray crystal structure now reveals that D-Trp enlarges the hydrophobic interaction, whereas *cyclo*-RGDpV cannot bind to the protein in a similar way without causing collisions between the D-Pro side chain and the integrin (Figure 7, top).

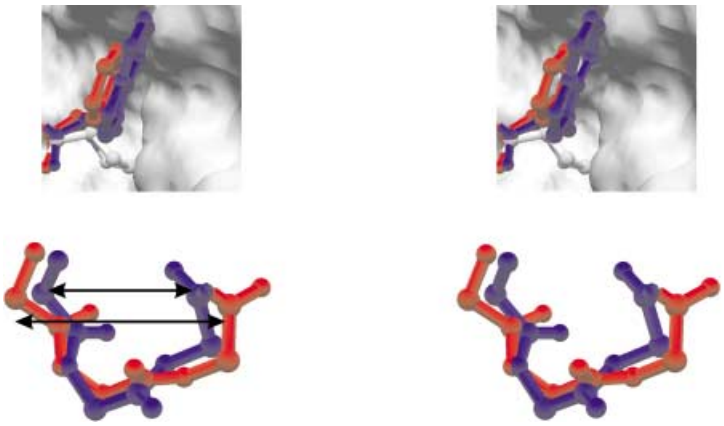

Figure 7. Effect of substitution on binding (stereoview). Top: Substitution of D-Phe (red) with D-Trp (blue) increases binding, but substitution of D-Phe with D-Pro (white) eliminates binding. This can now be easily explained in structural terms: whereas D-Trp increases the hydrophobic interaction, D-Pro overlaps with the protein (grey surface). Bottom: Effect of Methylation; in the nonmethylated form (blue) the C_α distance is shorter than in the methylated form (red).

N-Methylation of Val increases the binding affinity approximately fourfold. A comparison of the conformation of c(-RGDfV-)[27] and c(-RGDf[NMe]V-) shows that the conformation is altered; the distance between the C_α atoms of Arg and Asp is shorter in the *N*-methylated than in the nonmethylated ligand (Figure 7, bottom).

7. Specificity of Interaction

As the only residue that is in contact with the α subunit is Arg, subunit specificity between different α subunits can only be achieved by different orientations of this side chain relative to the aspartic acid residue, by variations of the arginine moiety, or by secondary effects, for example, structural changes in the β subunit induced by different α subunits. Ligand-design studies have shown an involvement of Arg in subunit specificity. On the one hand, it was demonstrated that replacing Arg by Lys leads to a loss in binding to $\alpha_v\beta_3$, but not to $\alpha_{IIb}\beta_3$. On the other hand, the guanidinium group of the arginine residue can be substituted with aminopyridine and

  1433-7851/02/4120-3770 $ 20.00+.50/0

other Arg mimetics without loss of binding to $\alpha_v\beta_3$, whereas the same substitution is not tolerated with $\alpha_{IIb}\beta_3$[14]. These data led to the basic assumption that Arg is bound side-on in $\alpha_v\beta_3$, but end-on in $\alpha_{IIb}\beta_3$. Indeed, the X-ray crystal structure reveals the validity of this assumption: Asp218 shows a side-on interaction with Arg; further stabilization occurs through Asp150 (Figure 8a).

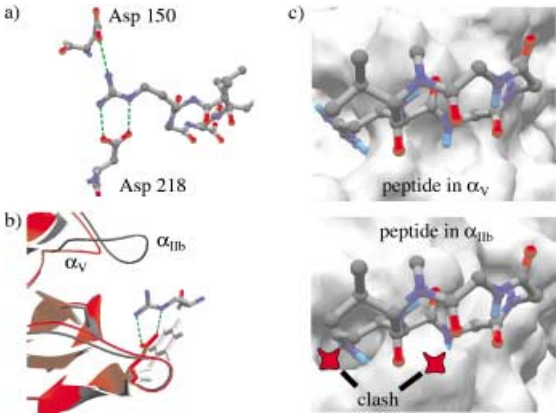

Figure 8. Comparison between $\alpha_v\beta_3$ and $\alpha_{IIb}\beta_3$. a) Binding of Arg: the Arg of the c(-RGDf[NMe]V-) is stabilized mainly by a side-on interaction of Asp218 of the α-subunit, in combination with an end-on interaction with Asp150 of the α subunit. b) A homology model of α_{IIb} superimposed on α_v reveals, that (α_v)-Asp218 is not conserved among the intergins. The corresponding residue is a Phe in α_{IIb}, rendering a side-on stabilization impossible. The residue which corresponds to Asp150 is a Glu, enabling an end-on interaction. The respective loop is also not conserved in the two integrins: in α_{IIb} (grey) the loop is longer, blocking the binding pocket. c) Whereas in α_v the peptide can insert the Arg into a negatively charged pocket of the protein (top), this pocket is much smaller for α_{IIb} (bottom), inducing an overlap between Arg and the protein. Further clashes between Gly and α_{IIb} increase the specificity of this ligand for α_v.

Sequence alignment shows that Phe231 of α_{IIb} corresponds to Asp218 of α_v. α_{IIb}-Phe231 cannot stabilize the Arg of the RGD ligand by side-on binding (Figure 8b). The residue that corresponds α_v-Asp150 is α_{IIb}-Glu157, which might serve as an end-on binding partner for Lys. An homology model of α_{IIb} (unpublished results) superimposed on α_v reveals that the α_v-specific RGD ligand is not suited to bind α_{IIb} in the same orientation as in α_v. The loop at the C terminus of α_v – Asp150 or α_{IIb} – Glu157 is not conserved between the two integrin subtypes. The longer loop of α_{IIb} closes the pocket in which c(-RGDf[NMe]V-) binds to α_v. Further steric clashes occur between G in RGD and the surface of α_{IIb} (Figure 8C). The X-ray crystal structure can thus not only rationalize different binding affinities of RGD-based ligands to $\alpha_v\beta_3$, but it can also help to understand different subtype specificities.

8. Models of Signal Transduction

Electron-microscopy (EM) images have led to the conclusion that the structural changes observed in ligand binding are not the final answer to questions regarding signal transduction. It has been shown in a number of studies that major structural rearrangements occur after the ligand-binding event[5, 28–32] which are not seen in the crystal structures of the extracellular domains. Depending on the nature of the experiments, two models of signal transduction have been developed and further refined (Figure 9).[28, 31] Both models

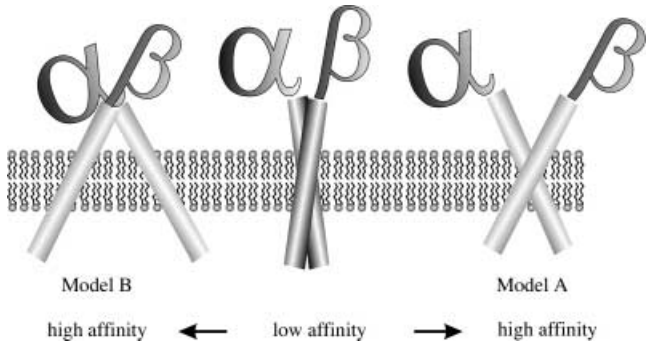

Figure 9. Two models for signal transduction by integrins. Whereas in Model A (right) the TM parts of the integrin subunits stay associated, in Model B (left) the hinge region is closer to the extracellular head group and the TM region is separated.

show that a scissorlike movement takes place, but they differ in the location of the hinge region. Whereas in the one model (model A) the hinge region is located in the membrane, the other model (model B) postulates a hinge region close to the head groups of the integrin. In model A the head groups dissociate after ligand binding, whereas in model B they remain associated. Recently model B has been refined and information has been incorporated from the X-ray crystal structure and further NMR spectroscopic studies of the stalk domains. Now a combination of a scissorlike movement with a switchbladelike opening of the kinked integrin structure has been proposed (Figure 10).[33] This model would explain

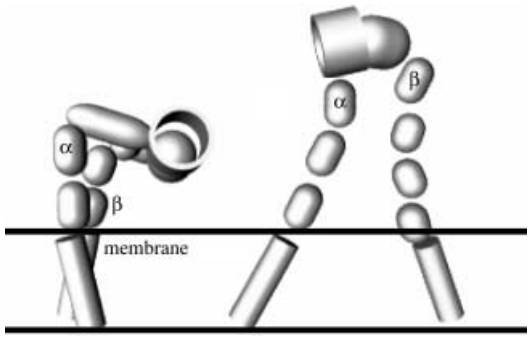

Figure 10. Swichtbladelike opening of integrins. This model of signal transduction has been derived by a combination of an analysis of the X-ray crystal structure, EM pictures, and NMR spectroscopic experiments of the stalk region of integrins. It is also in agreement with sedimentation experiments.

sedimentation experiments, which demonstrate an enlargement of the hydrodynamic radius of the integrin after ligand binding. These sedimentation data are also in accordance with the model with dissociating head groups. The available EM data are contradictory and do not allow a clear distinction between the two models. There is evidence for both models.[7, 28, 34–37]

  1433-7851/02/4120-3771 $ 20.00+.50/0

Whereas model A was derived from whole integrins, model B used a construct in which the activation step consisted of the cleavage of one of the TM domains from the integrin. Although it is known that cleavage of the TM domains does activate the integrin, the removal of the structural restraints provided by the membrane might possibly affect the validity of the model. It has been shown by previous EM investigations that cleavage of the TM domains does not lead to a dissociation of the head groups,[38] whereas addition of ligand does.[7, 28] On the other hand, there are many investigations in which dissociation of the head groups has not been described.[34]

Biochemical studies demonstrated recently that the activation process is not a two-step, but rather a multistep process, which most probably consists of three states.[39, 40] This is corroborated by extensive computational studies of the TM domains of a large number of different integrin subtypes.[41] Two conformations (a high- and a low-affinity conformation) of the TM regions have been identified based on the calculations in combination with experimental data. The high-affinity conformation of integrins is similar to the structure of glycophorin A,[42] a homodimeric glycoprotein.

A calculated pathway between these two conformations revealed the existence of a third state and a rather complex movement of the helices during the transition. The activating movement is a rotation of the helix of the α subunit; the dissociation is accompanied by a back rotation of the α subunit to approximately the initial rotation angle, by an increase in the tilt angle between the helices and by a rotation of the β subunit. How these TM movements are translated to movements of the head groups is not clear. It has been postulated that this newly introduced intermediate is an activated state, which corresponds to the crystal structure without the TM and intracellular domains.[41] The crystal structure should represent an activated form for a variety of reasons:

1) The TM and intracellular domains are missing, which has been shown to render the integrin active.[5]
2) The substitution of Ca^{2+} by Mg^{2+} ions, which also activates the integrin, does not change the structure.[5, 16, 43]
3) The structural changes after ligand binding are minor; nevertheless the head groups are still associated.

These observations corroborate the conclusion drawn from the computational studies that activation does not dissociate the head groups, but rather alters their relative orientation. Although the computational studies are in agreement with a scissorlike movement of the two subunits, the conformational change of the TM domains might also induce a rearrangement of disulfide bridges in the stalk region, which would be in accordance with the switchbladelike opening model.

A possible mechanism of dissociation of the head groups after ligand binding involves the central residue at the α/β interface, the Arg261 of the β subunit.[6] Two loops that alter their conformation upon ligand binding are close to (β)-Arg261. (β)-Arg261 inserts into the β propeller of the α subunit. It is surrounded by aromatic residues of the β propeller domain of α_v (Figure 2). Thus, cation–π interactions should contribute to the stabilization of the α/β interface.[6] A slight change in the position of (β)-Arg261 induced by allosteric rearrangement caused by ligand binding can lead to repulsive cation–π interactions.[44] This might initiate the dissociation of the head groups. The dissociation event may either not take place if the ligands are cyclic RGD peptides, or it might be inhibited by the crystallization or soaking conditions. It is not yet clear where the RGD peptide binds after dissociation of the head groups. One possible mechanism would be that Arg of the RGD peptide replaces (β)-Arg261 and binds to the β-propeller domain, thus inhibiting a reassociation of the head groups.

9. Clustering

Transduction of signals into the cell after ligand binding is accompanied by clustering of integrins. This effect is partially regulated by interactions of integrins with other membrane-spanning proteins such as calveolin, the urokinase receptor (uPAR = CD87), and others.[45–48] Whether integrins interact directly in the clustering process or are only connected through their ligands or through other proteins to the cell surface is unknown. Recently, a short peptide sequence in the β-propeller domain of the α_3 subunit has been identified which inhibits $\alpha_3\beta_2$–uPAR interactions (Figure 2).[45] The corresponding loop is occluded by the β subunit in the crystal structure. To be involved in integrin–uPAR interaction, dissociation of the head groups has to occur to expose the loop, provided that the $\alpha_3\beta_2$ integrin adopts a similar structure as $\alpha_v\beta_3$ (Figure 11). These experiments in connection with the structural data available strongly corroborate the notion that the integrin head groups have to dissociate for clustering to occur. Crosslinks with other membrane-spanning receptors such as the human growth factor has also been observed.[49, 50]

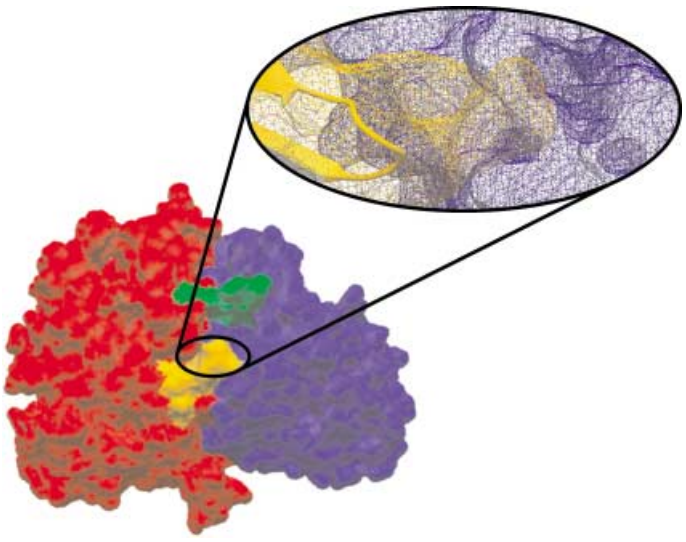

Figure 11. Interaction of integrins with uPAR. A loop located in the β propeller domain of α_3 has been identified to interact with uPAR. The β propeller domain of the α subunit is shown in red, with the surface of the bound ligand shown in green. The surface of the β subunit is shown in blue. The corresponding loop that interacts with uPAR (orange) is close to the ligand (green) and partially occluded by the β-subunit (blue surface and inset). To interact with uPAR, the head groups of the respective integrin have to dissociate.

  1433-7851/02/4120-3772 $ 20.00+.50/0

Even direct interactions between integrins can in principle occur at all domains. One model for these direct interactions is that one domain of the dissociated head groups of one integrin dimer make place for the respective counterpart of another integrin dimer. But the studies on $\alpha_2\beta_3$–uPAR interactions rather imply that the head groups serve as interaction regions for other membrane-associated receptors, which in turn induce clustering of integrins. EM images imply a possible mechanism in which the stalk regions of integrins may interact in the absence of other proteins.[37]

10. Emerging Themes in Signal Transduction

Closer investigation of the signal transduction mechanism of integrins and the interplay of G proteins and G-coupled proteins reveal conceptual similarities, which might indicate a common general mechanism for signal transduction events (Figure 12). In both cases an inactive conformation exists,

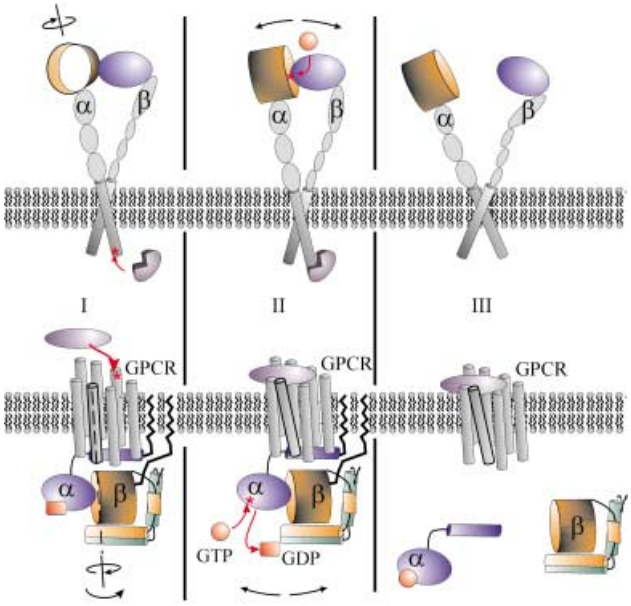

Figure 12. Conceptual similarity of signal transduction with integrins and G-coupled receptors. In both cases a ligand induces a reorientation of the TM helices (panel I). This conformational change is transduced to another ligand binding domain at the other side of the membrane, allowing binding or exchange of ligand (panel II). Binding of the second ligand induces separation of two domains close to the binding site (panel III). This separation can be the starting point for further signal cascades.

which is activated by intra- or extracellular signals. In the case of integrins, this activation appears to be a rotation of one of the subunits, as concluded from computational studies.[41] In G-coupled proteins, the activation step also includes the structural reorientation of helices (Figure 12, I).[51–57]

The conformational change is followed in the case of integrins by the binding of extracellular ligands,[5] in the case of G-coupled receptors it leads to replacement of GDP with GTP (Figure 12, II).

Binding of ligands or replacement of GDP with GTP induces further structural changes, which in both cases involve the dissociation of proteins or protein domains: In integrin signal transduction, the head groups dissociate,[28] whereas in G proteins, the α subunits dissociate from the $\beta\gamma$ complex (Figure 12, III).[58] In this case, the conceptual similarity is reflected by a striking structural similarity: the interfaces of the interaction domains resemble each other very much.[6, 59, 60] Cation–π interactions stabilize the interface for $\alpha_v\beta_3$, but not for G proteins. For G proteins, a network of salt bridges leads to strong interactions. Cation–π interactions are very well-suited to regulate the affinity of two domains for each other: small structural changes can render the attractive force repulsive, thus leading to dissociation of the respective domains. Dissociation of the domains is the starting point for a cascade of further events. For integrins, the final step in signal transduction is comprised of interaction with other receptors and cluster formation.[50] The common theme which emerges is a mechanism that comprises three states (inactive, activated, dissociated), possibly followed by clustering.

11. Conclusion and Outlook

The recent studies of integrin $\alpha_v\beta_3$ and other integrins have led to a new understanding of ligand binding to integrins and of signal transduction by integrins. Nevertheless, many questions regarding further structural changes after ligand binding and dynamical processes, for example, interactions with further proteins and cluster formation remain unanswered. The structures of integrin $\alpha_v\beta_3$ in the free form as well as in complex with a cyclic RGD ligand are certainly hallmarks in integrin research. They will stimulate research both by medicinal chemists as well as by biophysicists and biochemists. The aim of the different research will be to develop highly potent integrin antagonists by rational protein-structure-based design and to improve the understanding of signal transduction and cell adhesion mediated by integrins.

Received: May 6, 2002 [M1570]

[1] A. E. Aplin, A. K. Howe, R. L. Juliano, *Curr. Opin. Cell. Biol.* **1999**, *11*, 737.
[2] K. H. Martin, J. K. Slack, S. A. Boerner, C. C. Martin, J. T. Parsons, *Science* **2002**, *296*, 1652.
[3] C. C. Kumar, L. Armstrong, Z. Yin, M. Malkowski, E. Maxwell, H. Ling, B. Yaremko, M. Liu, J. Varner, E. M. Smith, B. Neustadt, T. Nechuta, *Adv. Exp. Med. Biol.* **2000**, *476*, 169.
[4] G. P. Curley, H. Blum, M. J. Humphries, *Cell Mol. Life Sci.* **1999**, *56*, 427.
[5] M. J. Humphries, *Biochem. Soc. Trans.* **2000**, *28*, 311.
[6] J. P. Xiong, T. Stehle, B. Diefenbach, R. Zhang, R. Dunker, D. L. Scott, A. Joachimiak, S. L. Goodman, M. A. Arnaout, *Science* **2001**, *294*, 339.
[7] J. W. Weisel, C. Nagaswami, G. Vilaire, J. S. Bennett, *J. Biol. Chem.* **1992**, *267*, 16637.
[8] M. A. Dechantsreiter, E. Planker, B. Mathä, E. Lohof, G. Hölzemann, A. Jonczyk, H. Kessler, *J. Med. Chem.* **1999**, *42*, 3033.
[9] J. P. Xiong, T. Stehle, R. Zhang, A. Joachimiak, M. Frech, S. L. Goodman, M. A. Arnaout, *Science* **2002**, *296*, 151.
[10] R. Haubner, R. Gratias, B. Diefenbach, S. L. Goodman, A. Jonczyk, H. Kessler, *J. Am. Chem. Soc.* **1996**, *118*, 7461.
[11] J. Wermuth, S. L. Goodman, A. Jonczyk, H. Kessler, *J. Am. Chem. Soc.* **1997**, *119*, 1328.
[12] K. E. Gottschalk, R. Gunther, H. Kessler, *ChemBioChem* **2002**, *3*, 470.

  1433-7851/02/4120-3773 $ 20.00+.50/0

[13] M. Pfaff, K. Tangemann, B. Müller, M. Gurrath, G. Müller, H. Kessler, R. Timpl, J. Engel, *J. Biol. Chem.* **1994**, *269*, 20233.
[14] S. L. Goodman, G. Hölzemann, G. A. G. Sulyok, H. Kessler, *J. Med. Chem.* **2002**, *45*, 1045.
[15] J. Boer, D. Gottschling, A. Schuster, M. Semmrich, B. Holzmann, H. Kessler, *J. Med.Chem.* **2001**, *44*, 2586.
[16] D. D. Hu, C. F. Barbas, J. W. Smith, *J. Biol. Chem.* **1996**, *271*, 21745.
[17] E. C. Tozer, R. C. Liddington, M. J. Sutcliffe, A. H. Smeeton, J. C. Loftus, *J. Biol. Chem.* **1996**, *271*, 21978.
[18] S. Honda, Y. Tomiyama, N. Pampori, H. Kashiwagi, T. Kiyoi, S. Kosugi, S. Tadokoro, Y. Kurata, S. J. Shattil, Y. Matsuzawa, *Blood* **2001**, *97*, 175.
[19] J. D. Humphries, J. A. Askari, X. P. Zhang, Y. Takada, M. J. Humphries, A. P. Mould, *J. Biol. Chem.* **2000**, *275*, 20337.
[20] J. Emsley, C. G. Knight, R. W. Farndale, M. J. Barnes, R. C. Liddington, *Cell* **2000**, *101*, 47.
[21] R. Haubner, D. Finsinger, H. Kessler, *Angew. Chem.* **1997**, *109*, 1440; *Angew. Chem. Int. Ed. Engl.* **1997**, *36*, 1374.
[22] G. Hölzemann, *IDrugs* **2001**, *4*, 72.
[23] E. Plancker, H. Kessler, unpublished results.
[24] M. Gurrath, G. Müller, H. Kessler, M. Aumailley, R. Timpl, *Eur. J. Biochem.* **1992**, *210*, 911.
[25] M. Pfaff, K. Tangemann, B. Müller, M. Gurrath, G. Müller, H. Kessler, R. T. J. Engel, *J. Biol. Chem.* **1994**, *269*, 20233.
[26] H. Kessler, *Angew. Chem.* **1982**, *94*, 509; *Angew. Chem. Int. Ed. Engl.* **1982**, *21*, 512.
[27] M. Aumailley, M. Gurrath, G. Müller, J. Calvete, R. Timpl, H. Kessler, *FEBS Lett.* **1991**, *291*, 50.
[28] R. R. Hantgan, C. Paumi, M. Rocco, J. W. Weisel, *Biochemistry* **1999**, *38*, 14461.
[29] R. C. Liddington, L. A. Bankston, *Exp. Cell Res.* **2000**, *261*, 37.
[30] C. Lu, J. Takagi, T. A. Springer, *J. Biol. Chem.* **2001**, *276*, 14642.
[31] J. Takagi, H. P. Erickson, T. A. Springer, *Nat. Struct. Biol.* **2001**, *8*, 412.
[32] E. F. Plow, T. A. Haas, L. Zhang, J. Loftus, J. W. Smith, *J. Biol. Chem.* **2000**, *275*, 21785.
[33] N. Beglova, S. C. Blacklow, J. Takagi, T. A. Springer, *Nat. Struct. Biol.* **2002**, *9*, 282.
[34] E. M. Erb, K. Tangemann, B. Bohrmann, B. Muller, J. Engel, *Biochemistry* **1997**, *36*, 7395.
[35] J. Engel, *Methods Enzymol.* **1994**, *245*, 469.
[36] X. Du, M. Gu, J. W. Weisel, C. Nagaswami, J. S. Bennett, R. Bowditch, M. H. Ginsberg, *J. Biol. Chem.* **1993**, *268*, 23087.
[37] R. R. Hantgan, M. Rocco, C. Nagaswami, J. W. Weisel, *Protein Sci.* **2001**, *10*, 1614.
[38] J. Wippler, W. C. Kouns, E. J. Schlaeger, H. Kuhn, P. Hadvary, B. Steiner, *J. Biol. Chem.* **1994**, *269*, 8754.
[39] D. Boettiger, F. Huber, L. Lynch, S. Blystone, *Mol. Biol. Cell* **2001**, *12*, 1227.
[40] D. Boettiger, L. Lynch, S. Blystone, F. Huber, *J. Biol. Chem.* **2001**, *276*, 31684.
[41] K. E. Gottschalk, P. D. Adams, A. T. Brunger, H. Kessler, *Protein Sci.* **2002**, *11*, 1800.
[42] K. R. MacKenzie, J. H. Prestegard, D. M. Engelman, *Science* **1997**, *276*, 131.
[43] D. D. Hu, J. R. Hoyer, J. W. Smith, *J. Biol. Chem.* **1995**, *270*, 9917.
[44] J. P. Gallivan, D. A. Dougherty, *Proc. Natl. Acad. Sci. USA* **1999**, *96*, 9459.
[45] Y. Wei, J. A. Eble, Z. Wang, J. A. Kreidberg, H. A. Chapman, *Mol. Biol. Cell.* **2001**, *12*, 2975.
[46] Y. Wei, M. Lukashev, D. I. Simon, S. C. Bodary, S. Rosenberg, M. V. Doyle, H. A. Chapman, *Science* **1996**, *273*, 1551.
[47] Y. Wei, X. Yang, Q. Liu, J. A. Wilkins, H. A. Chapman, *J. Cell. Biol.* **1999**, *144*, 1285.
[48] H. T. Maecker, S. C. Todd, S. Levy, *FASEB J.* **1997**, *11*, 428.
[49] M. A. Schwartz, M. H. Ginsberg, *Nat. Cell. Biol.* **2002**, *4*, E65.
[50] C. K. Miranti, J. S. Brugge, *Nat. Cell. Biol.* **2002**, *4*, E83.
[51] S. W. Lin, T. P. Sakmar, *Biochemistry* **1996**, *35*, 11149.
[52] D. L. Farrens, C. Altenbach, K. Yang, W. L. Hubbell, H. G. Khorana, *Science* **1996**, *274*, 768.
[53] A. D. Jensen, F. Guarnieri, S. G. Rasmussen, F. Asmar, J. A. Ballesteros, U. Gether, *J. Biol. Chem.* **2001**, *276*, 9279.
[54] U. Gether, *Endocr. Rev.* **2000**, *21*, 90.
[55] U. Gether, B. K. Kobilka, *J. Biol.Chem.* **1998**, *273*, 17979.
[56] U. Gether, S. Lin, P. Ghanouni, J. A. Ballesteros, H. Weinstein, B. K. Kobilka, *EMBO J.* **1997**, *16*, 6737.
[57] S. Subramaniam, R. Henderson, *Nature* **2000**, *406*, 653.
[58] A. Bohm, R. Gaudet, P. B. Sigler, *Curr. Opin. Biotechnol.* **1997**, *8*, 480.
[59] M. A. Wall, B. A. Posner, S. R. Sprang, *Structure* **1998**, *6*, 1169.
[60] M. A. Wall, D. E. Coleman, E. Lee, J. A. Iniguez-Lluhi, B. A. Posner, A. G. Gilman, S. R. Sprang, *Cell* **1995**, *83*, 1047.

  1433-7851/02/4120-3774 $ 20.00+.50/0